Infectious Disease Modelling 10 (2025) 813–839

Contents lists available at ScienceDirect

Infectious Disease Modelling

journal homepage: www.keaipublishing.com/idm

Dynamics of an epidemic controlled by isolation and quarantine: A probability-based deterministic model

David V. Kalbaugh

33 N Pintail Dr, Ocean Pines, MD 21811, United States

ARTICLE INFO

Article history:
Received 14 January 2025
Received in revised form 11 March 2025
Accepted 12 March 2025
Available online 18 March 2025
Handling Editor: Dr Yijun Lou

ABSTRACT

Assuming a homogeneous population, we employ a deterministic model based on first principles of probability to explore dynamics of an epidemic controlled by isolation alone, quarantine alone, and the two together. We develop explicit closed-form equations for key metrics of control performance: cumulative fraction of population infected over the course of the epidemic (final size), maximum fraction infected at any one time, and epidemic duration. We derive an analytical solution for final size of an epidemic controlled by isolation, when final size is small, and develop empirical relations for the other cases. We frame equations in terms of reproduction numbers, measures of intervention effort and initial conditions. We model both strength and speed of interventions, assume second order gamma distributions for intervention waiting times and employ non-time-invariant equations for quarantine. We also account for quarantine of unexposed, susceptible individuals and for imperfect intervention.

1. Introduction

We begin with a thumbnail sketch of the history of mathematical epidemiology. Siettos and Russo (2013), Heesterbeck and Roberts (2015), Lessler and Cummings (2016) and Brauer (2017) are among more comprehensive histories of the subject prior to 2019.

In 1760 Daniel Bernoulli developed what is usually described as the first model in mathematical epidemiology when he analyzed inoculation against smallpox (Bernoulli, 1766; Blower, 2004; Heesterbeck & Roberts, 2015). Hamer (1906) proposed a *mass action law*, in which rate of new infections in a disease outbreak is proportional to the product of the number of susceptible individuals and the number of infected ones. Kermack and McKendrick (1927) incorporated the mass action law and introduced compartments to model spread of infectious diseases. A special case of their general model is referred to as the SIR model with compartments S (susceptible but well), I (infected and able to transmit the disease) and R (removed by immunity, recovery, death or quarantine). The SIR model is deterministic, meaning it incorporates no element of chance. In the late 1920's through the '40's L. Reed and W.H. Frost developed the stochastic Reed-Frost model. Stochastic models include the element of chance. The SIR and Reed-Frost models have been the starting points of many models developed since (Brauer; Lessler and Cummings (2016)).

E-mail address: davekalbaugh@gmail.com.
Peer review under the responsibility of KeAi Communications Co., Ltd.

https://doi.org/10.1016/j.idm.2025.03.007

Isolation is removal of an infected person from public interaction. *Quarantine* is removal of a segment of the population, regardless of health condition, usually by government order. Among many notable studies of quarantine and isolation using deterministic compartmental models are Hethcote et al. (2002) and Gumel et al. (2004).

For simplicity models often assume a homogeneous population, which means that all probabilities apply equally to all individuals. But spatial, age and demographic heterogeneity are real-life conditions that require additional model sophistication. The professional standard is set by immense computer programs that account for millions of people individually; their age, demographic status and location, with real data on such matters as airline schedules from city to city. Halloran et al. (2008); Ferguson et al. (2006); German et al. (2006) and Lewis et al. (2007) are examples of this so-called *agent-based* approach. Among many advantages of an agent-based approach is the opportunity to account for temporal dynamics of virus and antibody levels within an infected individual and more realistically model that individual's varying capacity to transmit the disease over time. See Xu et al. (2023).

In December 2019 a series of pneumonia cases of unknown cause emerged in Wuhan, China. (Huang, C. et al. (2020). The cause, the world soon learned, was a new virus that produced a disease eventually called COVID-19. The disease spread rapidly and became the most serious pandemic in over a century, wreaking havoc on the world's health and economy. Although use of mathematical modeling has for some time been standard practice at various levels of decision-making in some areas (Kretzschmar, 2020, Van Kerkhove and Ferguson, 2012, Metcalf et al., 2015, Heesterbeck, 2015), COVID-19 appears to have brought it to a level of global significance. Different nations relied on different models. The United Kingdom, e.g., depended in large part on an Imperial College London team that employs both an agent-based simulation as discussed above and a simpler but still large program with ordinary differential equations (ODEs) modeling transitions among compartments in sufficient number to capture key heterogeneities (Adam (2020)). (Brooks – Pollock et al. (2021) documents other modeling efforts that helped shape the early COVID 19 response in the UK.) Meanwhile the US's Center for Disease Control initially forwarded University of Washington projections based not on transmission dynamics but on a statistical curve-fitting model (Jewell et al. (2020)).

Addressing the challenge of COVID-19, journal articles modeling it have been published at a high rate. Many employed sophisticated methods. For example, Aleta et al. (2020) used a detailed, agent-based, stochastic, discrete-time simulation. Also using a detailed agent-based stochastic simulation, Kucharski et al. (2020) employed a contact model built on data previously collected on more than 40 thousand individuals. Peak et al. (2020) employed a stochastic branching model, and Huang et al. (2021) applied data-driven and machine-learning methods.

But response to COVID-19 also demonstrated the value of simple models: they enabled early, rough predictions of the epidemic's course and tentative assessments of candidate interventions. Many COVID-19 modeling efforts assumed a homogeneous population and adopted relatively simple deterministic compartmental models. Some of these collected local data and forecast the epidemic's spread in that locale, e.g., Gog and Hollingsworth (2021, in the UK), Giordano et al. (2020, in Italy), Sarkar and Nieto (2020, in India), Liu et al. (2020, in China) and Rainisch et al. (2020, in Chile).

Kalbaugh (2021) was also motivated by the COVID-19 epidemic but its purpose was to introduce a new form of deterministic model. Assuming a homogenous population, it applied quarantine-adjusted incidence (see, e.g., Hethcote et al. (2002)), a second order gamma distribution for recovery time and developed from first principles of probability an eighth-order deterministic system of ODEs to model effects of isolation and quarantine. The new model's major differences from typical compartmental models were its (1) incorporation of both strength and speed of interventions, which permits consideration of imperfect intervention, (2) use of second order gamma distributions for isolation and quarantine time to events, (3) employment of non-time-invariant ODEs for quarantine, and (4) accounting for quarantine removal of unexposed, susceptible individuals from circulation, which only a few past studies have done, among them Lipsitch et al. (2003), Muyabi (2010), Safi and Gumel (2013) and Sarkar and Nieto (2020).

This article follows on to Kalbaugh (2021). We develop explicit closed-form equations for key performance metrics for epidemics controlled by isolation, by quarantine, and by the two interventions together. As best we can determine, the literature has no other examples of this. This is surprising, given the large number of quantitative studies that have been published, but articles we have reviewed either report findings numerically or derive equations in implicit form. First to provide closed-form implicit equations for a controlled epidemic was Feng (2007). Using a compartmental model, that article provided equations for final size and for a quantity closely related to peak fraction of population infected. It addressed exponentially-distributed and gamma-distributed recovery times and also modeled imperfect isolation. We will compare our results to those of that article.

Outlining the rest of this article, Section 2 sketches briefly the basis for the model employed here. Section 3 addresses objectives in our development of empirical equations. Section 4 examines dynamics of epidemic spread when isolation is applied alone. It examines control performance when the epidemic is only just contained and when additional isolation effort is supplied. It quantifies key dynamic metrics: cumulative fraction of population infected over the course of the epidemic (often referred to as *final size*), peak fraction of population infected at any one time, and epidemic duration. It derives an analytical solution for final size in the isolation-only scenario when final size is small enough for equations to be linearized. Section 5 examines dynamics of epidemic spread when quarantine is applied alone. From first principles of probability, it derives new equations for quarantine dynamics, correcting an error in Kalbaugh (2021). Section 6 derives new equations for isolation and quarantine applied together, resulting in a 14th order system of ODEs. It then quantifies the key performance metrics for that scenario. Finally, Section 7 reviews main points of the article and adds pertinent observations.

2. Basis of the model

For the convenience of the reader this section briefly sketches the fundamental basis for the model employed here. Appendix A describes its underlying assumptions. Its mathematical derivation is described in more detail in following sections.

We define.

$p(t)$ = probability {person drawn randomly from population has been infected prior to time t}

$s(t)$ = prob{person is susceptible but well and not in quarantine at time t}

$i(t)$ = prob {person has been infected and is not recovered, isolated or quarantined at time t}

$r(t)$ = prob {person is recovered at time t}

$q_A(t)$ = prob {person is in quarantine at time t}

$q_B(t)$ = prob{person is in isolation at time t}.

The model is founded on four fundamental equations, together with use of probability theory to compute subsequent variables.

- the mass action law, which is the basis for the aforementioned, venerable SIR model:

$$\frac{dp}{dt} = \beta si \tag{1}$$

where β is the rate of disease spread by a single infected individual.

- The conditional probability that a person is recovered at time t given they were infected at time τ is defined to be

$$r(t|\tau) = 1 - (1 + \gamma_R(t-\tau))\exp(-\gamma_R(t-\tau)) \tag{2}$$

- The conditional probability that a person is in quarantine at time t, given that they have not been isolated, is defined to be

$$q_A(t) = q_{A0}[1 - (1 + \gamma_A t)\exp(-\gamma_A t)] \tag{3}$$

- The conditional probability that a person is in isolation at time t given they were infected at time τ and have not recovered is defined to be

$$q_B(t|\tau) = q_{B0}[1 - (1 + \gamma_B(t-\tau))\exp(-\gamma_B(t-\tau))] \tag{4}$$

In the above,

q_{A0} = prob{person is eventually quarantined, given that they were not isolated}

q_{B0} = prob{person is eventually isolated, given that they have not recovered}

We will refer to q_{A0} and γ_A as the *strength* and *speed* of the quarantine process, and q_{B0} and γ_B as the *strength* and *speed* of the isolation process. Nota bene that these terms do not reflect true effort the interventions require. Quarantine exacts a much greater cost on the economy and on personal liberty than does isolation.

Note that Eqs. (2)–(4) are second-order gamma distributions. The first order, or exponential, distribution has the attribute that the most likely time for completion of the process is just after it has begun, which is unrealistic, as discussed (for recovery) in Deikmann et al. (2013). For second and higher order gamma distributions, the most likely time of completion is well after the process has begun.

One can find examples in the literature of models assuming higher order gamma distributions for recovery time. As mentioned earlier, Feng (2007) is one of these. We have not found examples of higher order gamma distributions for isolation or quarantine wait times. As we will discuss, using probability theory for calculations involving second order distributions for isolation and quarantine times produces ODEs that are fundamentally different from those in the typical compartmental model.

Given the model's SIR basis and our use of the letters A to designate quarantine and B to designate isolation, for simplicity and brevity we shall refer to it as the SIRAB model.

3. Remarks on development of empirical equations

Our objective in this article is to develop explicit closed-form equations relating key control performance metrics to parameters quantifying isolation and quarantine effort. The performance metrics we focus on are final size (p_∞), i.e., fraction

of population ultimately infected at some time during the outbreak, given by the final value of $p(t)$; maximum fraction of population infected at any one time (i_{TMAX}), given by the peak value of $p(t) - r(t)$; and the outbreak's duration (T_E). The parametric measures of control effort are quarantine strength (q_{A0}), quarantine speed (γ_A), isolation strength (q_{B0}) and isolation speed (γ_B). (We again note that in achieving a given level of effort as defined above, quarantine exacts a much greater cost on the economy and on personal liberty than does isolation.) Other factors necessary in the equations are the epidemic's basic reproduction number (R_0), initial size (p_0) and an infected person's rate of recovery (γ_R). Initial size p_0 is set by the start of the intervention; it is an important variable in management of the epidemic; the earlier intervention is begun the better the outcome. In this study the unit of time is the mean time of recovery. For the SIRAB model, with its second-order recovery probability distribution, mean time of recovery is given by $2/\gamma_R$. Hence we set $\gamma_R = 2$.

With one notable exception the equations we develop are empirically derived. We derive an analytical solution for p_∞ in the isolation-only scenario when p_∞ is small. Otherwise, we develop empirical equations to stand in for difficult-to-obtain exact solutions.

We seek simple equations that reflect broad trends in the data. We hope that equations we develop will prove useful to epidemiologists seeking to understand basic dynamics of isolation and quarantine: how key performance metrics depend on parameters we can control and/or measure.

We seek to minimize error between numerical integration data and our equations, but not at the expense of simple expressions reflecting broad trends. It is possible to reduce error in an empirical equation to any desired level if the equation is evaluated only at data points used to create it. One can “tune” an empirical equation to fit a specific data base. When this is done results have nothing of the character of an ODE solution and are of no help to one interested in basic dynamics.

See Appendix B for details of the methodology employed.

4. Dynamics of epidemics controlled by isolation

This section explores dynamics of epidemic spread when controlled by isolation.

In Eq. (1) we need expressions for $s(t)$ and $i(t)$. Assuming no one is initially immune,

$$s(t) = 1 - p(t) \tag{5}$$

How does one compute the value of $i(t)$, the probability that an individual has been infected and is not recovered or isolated at time t? From the definitions above and probability theory,

$$i(t) = \int_0^t \dot{p}(\tau)(1 - r(t|\tau))(1 - q_B(t|\tau))d\tau \tag{6}$$

Given the forms of $r(t|\tau)$ and $q_B(t|\tau)$ in Eqs (2) and (4) above, with their $t - \tau$ arguments, Eq. (6) is equivalent to a set of linear time-invariant ODEs, which turn out to be

$$\begin{aligned}
\frac{di_B}{dt} &= (\gamma_R + \gamma_B)(i_{B1} - i_B) \\
\frac{di_{B1}}{dt} &= \left(\frac{\gamma_R^2 + \gamma_B^2}{\gamma_R + \gamma_B}\right) q_{B0} p + (\gamma_R + \gamma_B)(i_{B2} - i_{B1}) \\
\frac{di_{B2}}{dt} &= \left(\frac{2\gamma_R \gamma_B}{\gamma_R + \gamma_B}\right) q_{B0} p - (\gamma_R + \gamma_B) i_{B2}
\end{aligned} \tag{7}$$

and then

$$\begin{aligned}
i &= p - r - q_B \\
q_B &= i_B - q_{B0} r
\end{aligned} \tag{8}$$

As an aside, note the intuitive nature of Eq. (8): the fraction currently infected is the fraction who have been infected less the fraction who have recovered or been isolated.

Coefficients such as $2\gamma_R\gamma_B/(\gamma_R + \gamma_B)$ that arise naturally in the SIRAB model have no counterpart in other SIR-like models. The typical SIR-like model describes transitions with pairs of equations like $\dot{x}_i = -\gamma_{ij} x_i + \ldots$ and $\dot{x}_j = \gamma_{ij} x_i + \ldots$, where the rate γ_{ij} common to the pair is a parameter set by the analyst.

Similarly, the probability that a person is recovered at time t is given, via probability theory, by

$$r(t) = \int_0^t \dot{p}(\tau) r(t|\tau) d\tau, \tag{9}$$

which, using Eq. (2), leads to the ODEs

$$\begin{aligned} \frac{dr}{dt} &= \gamma_R (r_1 - r) \\ \frac{dr_1}{dt} &= \gamma_R (p - r_1) \end{aligned} \tag{10}$$

As an aside, note that Eqs. (6) and (9) are generic and that gamma distributions of any order could be employed in each case. This is important, e.g., because it has been established that different diseases have different recovery time distributions. Using higher order gamma distributions would result in a larger number of ODEs, which is not a high price to pay in today's numerical integration environment.

In total, the SIRAB model for control of an epidemic by isolation alone is

$$\begin{aligned} \frac{dp}{dt} &= \beta s i \\ s &= 1 - p \\ i &= p - r - q_B \\ q_B &= i_B - q_{B0} r \\ \frac{dr}{dt} &= \gamma_R (r_1 - r) \\ \frac{dr_1}{dt} &= \gamma_R (p - r_1) \\ \\ \frac{di_B}{dt} &= (\gamma_R + \gamma_B)(i_{B1} - i_B) \\ \frac{di_{B1}}{dt} &= \left(\frac{\gamma_R^2 + \gamma_B^2}{\gamma_R + \gamma_B} \right) q_{B0} p + (\gamma_R + \gamma_B)(i_{B2} - i_{B1}) \\ \frac{di_{B2}}{dt} &= \left(\frac{2\gamma_R \gamma_B}{\gamma_R + \gamma_B} \right) q_{B0} p - (\gamma_R + \gamma_B) i_{B2} \end{aligned} \tag{11}$$

In the SIRAB model, the effectiveness of isolation can be reliably predicted via the *isolation reproduction number* R_B, the expected number of cases directly generated by one infected person in a population where all other individuals are susceptible to infection and the epidemic is controlled by isolation alone.

For isolation alone, the infected individual's interaction with others is unaffected but his or her time in circulation is reduced. Given that the individual was infected at time $\tau = 0$, the probability he or she is still infectious and circulating at time t is $(1 - r(t|0))(1 - q_B(t|0))$. Then

$$R_B = \beta \int_0^\infty (1 - r(t|0))(1 - q_B(t|0)) dt \tag{12}$$

Using Eqs. (2) and (4) we eventually arrive at

$$R_B = \beta((1 - q_{B0})(2 / \gamma_R) + q_{B0} t_B) \tag{13}$$

where

$$t_B = \frac{2}{\gamma_R + \gamma_B} \left(1 + \frac{\gamma_R \gamma_B}{(\gamma_R + \gamma_B)^2} \right) \tag{14}$$

Setting $q_{BO} = 0$ in Eq. (13) reveals that $2\beta/\gamma_R$ is R_0, the basic reproduction number for the unmitigated epidemic. Hence Eq. (13) can be written

$$R_B = R_0\left[(1-q_{B0}) + q_{B0}\left(\frac{\gamma_R}{\gamma_R+\gamma_B}\right)\left(1+\frac{\gamma_R\gamma_B}{(\gamma_R+\gamma_B)^2}\right)\right] \tag{15}$$

This section will quantify p_∞, i_{TMAX} and T_E when $R_B \leq 1$.

4.1. Fundamentals of epidemic dynamics when controlled by isolation

We begin discussion of epidemic dynamics when controlled by isolation alone by examining the general character of the performance metrics as influenced by basic reproduction number and control parameters. That is, before focusing on equations we explore the qualitative nature of the dynamics, illustrating much of it graphically.

4.1.1. Final size: isolation-only

Numerical integration and analysis show that, when an epidemic is controlled by isolation alone, final size p_∞ is a function of initial size p_0 and isolation reproduction number R_B only.

Fig. 1 plots final size p_∞ as a function of R_B, with p_0 as a parameter. Note that setting $R_B = 1$, where R_B is as defined in Eq. (15), accurately predicts the division between containment and breakout of an epidemic. Although it is difficult to find another name for the opposite of "breakout", "containment" is, in a sense, too strong a word. According to the SIRAB model, as shown in Fig. 1, p_∞ is much larger than p_0 unless R_B is considerably less than one. More isolation effort brings much reward.

4.1.2. Peak fraction of population infected: isolation-only

The variable i_{TMAX}, the maximum fraction of population infected at any one time, is a measure of the epidemic's stress on medical facilities. We find that i_{TMAX} is proportional to p_0. This again points to the importance of early intervention in the course of an epidemic. Note that this result, which applies when $R_B < 1$, is in strong contrast to the case where $R_B > 1$ and the epidemic is not contained. In that case i_{TMAX} is essentially independent of p_0.

Numerical results show that, when isolation is the only control, i_{TMAX} depends primarily on R_0, with R_B and γ_B having secondary influence. Fig. 2 is an example. The relatively weak dependence of i_{TMAX} on R_B sets the metric apart from p_∞ and, as we will see shortly, T_E.

4.1.3. Epidemic duration: isolation-only

We can better understand duration of an epidemic controlled only by isolation if we examine in some detail a few specific examples. Fig. 3 graphs the time history of $i(t)$, the fraction of circulating population infected at that time, for a few representative cases. Each curve represents the history of $i(t)$ for a particular value of R_B. As $R_B \to 1$, the $i(t)$ curves flatten out; isolation is containing the epidemic but not suppressing it.

To quantify duration of these simulated epidemics we must decide on a criterion for when an epidemic can be said to be extinguished. We choose to set a threshold i_E on the fraction of the circulating public that is infected. Other criteria could be

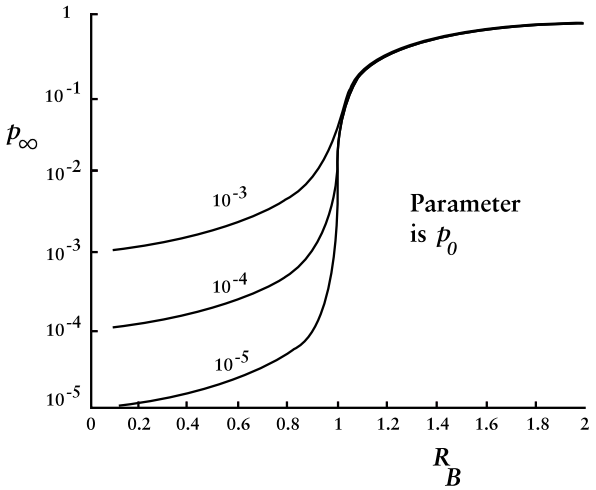

Fig. 1. Final size p_∞ as function of isolation reproduction number R_B.

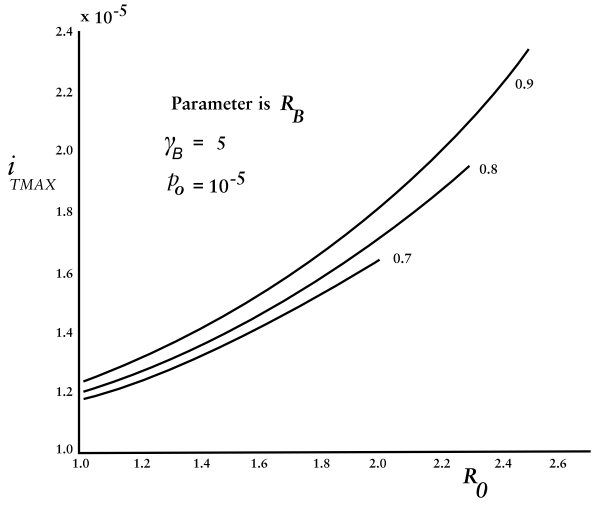

Fig. 2. Peak fraction of population infected i_{TMAX} versus basic epidemic reproduction number R_0, with isolation reproduction number R_B as parameter.

chosen. Also, any value we choose for the threshold i_E is somewhat arbitrary. As it happens, the empirical equations we develop for T_E will sidestep this issue by keeping i_E as a parameter. However, to quantify the duration of the simulated epidemics graphed in Fig. 3 we must decide on a firm criterion. Somewhat arbitrarily, we set $i_E = 10^{-3}p_0$.

Fig. 4 depicts duration of epidemics simulated in Fig. 3 and shows sensitivity to p_0. Rapid growth in duration occurs for all p_0 as $R_B \to 1$. If isolation is the only intervention measure, R_B must be at least 10 percent less than unity for epidemic duration to be reasonable. Picking up from our earlier discussion of increasing isolation effort to limit p_∞, we see that another objective is to limit T_E.

A reviewer has made the interesting observation that the slowing of dynamics evidenced by the lengthening of epidemic duration as $R_B \to 1$ in Fig. 4 is similar to behavior seen in other systems with phase transitions. The reviewer suggests Stauffer and Aharony (2018), Baxter et al. (2015), Zhang et al. (2018), and Baronchelli (2007), for readers interested in investigating this connection further.

4.2. Equations for isolation performance metrics

This section focuses on explicit closed-form equations describing the performance metrics p_∞, i_{TMAX} and T_E as a function of isolation strength q_{B0}, isolation speed γ_B, initial size p_0 and R_0.

4.2.1. Equation for final size: isolation-only

In this paper the one exception to an empirical approach is the equation for final size (p_∞) when isolation is applied alone. In this subsection we show that, provided $p_0 \ll 1 - R_B$, the analytical solution to Eq. (11) is

$$p_\infty = \lim_{t\to\infty} p(t) = \frac{p_0}{1 - R_B} \tag{16}$$

First, we assume $p \ll 1$, in which case $s \cong 1$ and we can write Eq. (11) in the form

$$\dot{\underline{x}} = \underline{A}\underline{x} \tag{17}$$

where

$$\underline{x} = \begin{pmatrix} p \\ r \\ r_1 \\ i_B \\ i_{B1} \\ i_{B2} \end{pmatrix} \tag{18}$$

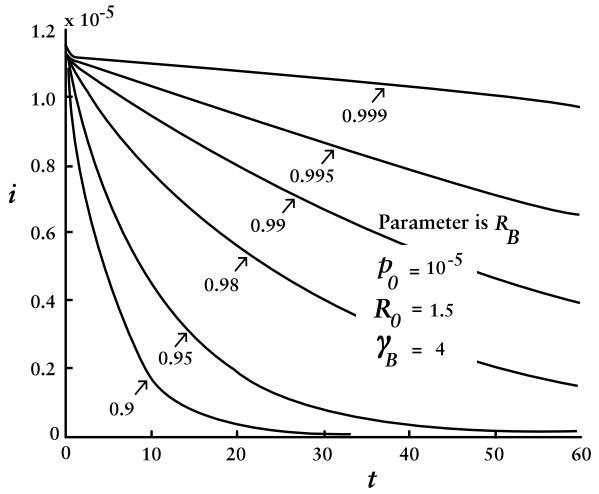

Fig. 3. Showing i, the fraction of circulating population infected as a function of time, with isolation number R_B as a parameter.

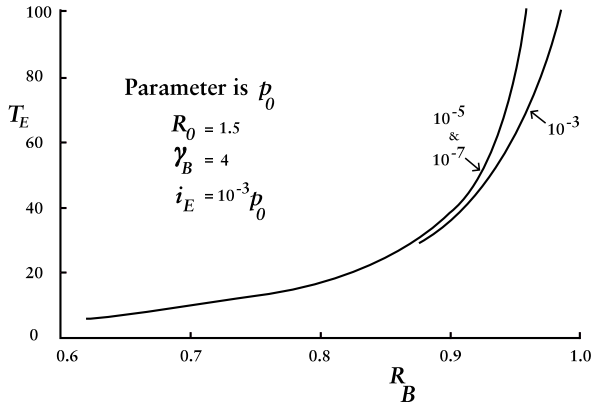

Fig. 4. Plotting duration T_E of example simulated epidemics as a function of isolation reproduction number R_B.

$$\underline{A} = \begin{pmatrix} \beta & -(1-q_{B0})\beta & 0 & -\beta & 0 & 0 \\ 0 & -\gamma_R & \gamma_R & 0 & 0 & 0 \\ \gamma_R & 0 & -\gamma_R & 0 & 0 & 0 \\ 0 & 0 & 0 & -(\gamma_R+\gamma_B) & \gamma_R+\gamma_B & 0 \\ q_{B0}\left(\frac{\gamma_R^2+\gamma_B^2}{\gamma_R+\gamma_B}\right) & 0 & 0 & 0 & -(\gamma_R+\gamma_B) & \gamma_R+\gamma_B \\ q_{B0}\left(\frac{2\gamma_R\gamma_B}{\gamma_R+\gamma_B}\right) & 0 & 0 & 0 & 0 & -(\gamma_R+\gamma_B) \end{pmatrix} \tag{19}$$

Next, we take the Laplace transform of Eq. (17), defining

$$\hat{\underline{x}}(s) = L\{\underline{x}(t)\} = \int_0^\infty \exp(-st)\underline{x}(t)dt \tag{20}$$

Now

$$L\{\dot{\underline{x}}(t)\} = s\widehat{\underline{x}}(s) - \underline{x}_0 \tag{21}$$

We assume an initial condition

$$\underline{x}_0 = \begin{pmatrix} p_0 \\ 0 \\ 0 \\ 0 \\ 0 \\ 0 \end{pmatrix} \tag{22}$$

Then

$$(s\underline{I} - \underline{A})\widehat{\underline{x}}(s) = \underline{x}_0 \tag{23}$$

$$\widehat{\underline{x}}(s) = (s\underline{I} - \underline{A})^{-1}\underline{x}_0 \tag{24}$$

A tedious but straightforward calculation results in

$$\widehat{p}(s) = \widehat{x}_1(s) = \frac{(s+\gamma_R)^2(s+\gamma_R+\gamma_B)^3}{D(s)}p_0 \tag{25}$$

where

$$\begin{aligned} D(s) &= \left(s^5 + a_4 s^4 + a_3 s^3 + a_2 s^2 + a_1 s + a_0\right)s \\ a_4 &= 5\gamma_R + 3\gamma_B - \beta \\ a_3 &= 10\gamma_R^2 + 12\gamma_R\gamma_B + 3\gamma_B^2 - \beta(5\gamma_R + 3\gamma_B) \\ a_2 &= (\gamma_R+\gamma_B)\left(10\gamma_R^2 + 8\gamma_R\gamma_B + \gamma_B^2\right) - \beta\left[3(\gamma_R+\gamma_B)(3\gamma_R+\gamma_B) - q_{B0}\gamma_B^2\right] \\ a_1 &= \gamma_R(\gamma_R+\gamma_B)^2(5\gamma_R+2\gamma_B) - \beta\left[7\gamma_R^3 + 15\gamma_R^2\gamma_B + (9-5q_{B0})\gamma_R\gamma_B^2 + \gamma_B^3(1-q_{B0})\right] \\ a_0 &= \gamma_R^2(\gamma_R+\gamma_B)^3(1-R_B) \end{aligned} \tag{26}$$

where, from Eq. (15)

$$R_B = R_0\left[(1-q_{B0}) + q_{B0}\left(\frac{\gamma_R}{\gamma_R+\gamma_B}\right)\left(1 + \frac{\gamma_R\gamma_B}{(\gamma_R+\gamma_B)^2}\right)\right] \tag{27}$$

and, again,

$$R_0 = \frac{2\beta}{\gamma_R} \tag{28}$$

Finally, we apply the Laplace transform final value theorem, which states that

$$p_\infty = \lim_{t\to\infty} p(t) = \lim_{s\to 0} s\widehat{p}(s) \tag{29}$$

provided a limit exists. From Eqs. (25), (26) and (29) we find that

$$p_\infty = \lim_{s\to 0} s\frac{(s+\gamma_R)^2(s+\gamma_R+\gamma_B)^3}{D(s)}p_0 = \frac{p_0}{1-R_B} \tag{30}$$

as was to be shown.

The larger the value of p_∞ , the larger the error in Eq. (30). Its absolute relative error is less than 0.6 percent provided $R_B \leq 0.9$ and $p_0 \leq 10^{-4}$. An empirically derived extension to take into account nonlinear effects is

$$p_\infty = \frac{p_0}{(1-R_B) + 0.5(p_0/(1-R_B)) - 4.1(p_0/(1-R_B))^2} \tag{31}$$

which has an error less than one percent when $R_B \leq 0.98$ and $p_0 \leq 10^{-3}$.

It is of interest to compare Eq. (30) to the implicit equation derived in Feng (2007). We must first recognize that the definition of final size in that article differs from the definition in this one. In this article final size is defined as the total fraction of individuals infected over the course of the epidemic. Feng (2007) defined it (under the assumption that no one is initially immune) as the difference between that total and the fraction of those who had already been infected at the start of intervention. In the notation of this paper, Feng's equation when isolation is applied alone is

$$p_\infty = 1 - (1-p_0)\exp(-R_B p_\infty) \tag{32}$$

Eq. (32) applies for exponentially-distributed and all orders of gamma-distributed recovery times though the form of R_B differs in each case.

We first observe that, with rearrangement and transformations $y = R_B(p_\infty - 1)$ and $x = R_B \exp(-R_B)(p_0 - 1)$, Eq. (32) can be written as

$$y \exp(y) = x, \tag{33}$$

the solution $y(x)$ of which is the well-known Lambert W function. For our purposes, however, it is more convenient to work directly with Eq. (32).

Assuming $R_B p_\infty \ll 1$ we can approximate

$$\exp(-R_B p_\infty) \cong 1 - R_B p_\infty \tag{34}$$

and then, assuming $p_0 \ll 1$, quickly determine that

$$p_\infty = \frac{p_0}{1-R_B} \tag{35}$$

Eqs. (30) and (35) have the same form.

Moreover, many trials over a wide range of R_B and p_0 values show that, within numerical uncertainty, p_∞ as computed from numerical integration of Eq. (11) and p_∞ as computed from iterative digital solution of Eq. (32) agree. That is, within numerical uncertainty, when isolation is the lone intervention, the SIRAB model satisfies Feng's implicit equation.

Feng derived the equation for a family of SEIR compartmental models. As we have said, Eq. (11) differ from typical compartmental models in various ways. That Feng's equation apparently applies to Eq. (11) as well indicates it has broader applicability.

Eqs. (30) and (31) do not cover the case where $R_B = 1$. Accepting that the SIRAB model satisfies Eq. (32), we can expand Eq. (32) when $R_B = 1$ using

$$\exp(-p_\infty) \cong 1 - p_\infty + (1/2)p_\infty^2 \tag{36}$$

and determine that, when $p_0 \ll 1$, final size can be approximated as

$$p_\infty = \sqrt{2p_0} \tag{37}$$

The absolute relative error in Eq. (37) is less than 1.5 % for $p_0 \leq 10^{-3}$.

To find a better estimate of final size for larger values of initial size when $R_B = 1$ we can:

(1) Expand Eq. (32) using

$$\exp(-p_\infty) \cong \sum_{n=0}^{N+1} (-p_\infty)^n / n! \tag{38}$$

(2) Express p_∞ as

$$p_\infty = \sum_{n=1}^{N} k_n (2p_0)^{n/2} \tag{39}$$

(3) Collect terms to write Eq. (32) as

$$\sum_{m=2}^{N+1} c_m(k_1, .., k_N)(2p_0)^{m/2} = 0 \tag{40}$$

ignoring higher order terms.

(4) Solve for k_n, $1 \le n \le N$, recognizing we must have

$$c_m(k_1, .., k_N) = 0, \quad 2 \le m \le N+1 \tag{41}$$

The results for $N = 4$ are

$$\begin{aligned} k_1 &= 1 \\ k_2 &= -1/3 \\ k_3 &= 11/72 \cong 0.15278 \\ k_4 &= -43/540 \cong -0.079630 \end{aligned} \tag{42}$$

Using these values for k_n, the absolute relative error in Eq. (39) is less than 0.7 % for $p_0 \le 0.2$.

If one decides that an epidemic is well contained when final size is less than X times initial size, then, from Eq. (35), R_B must satisfy

$$R_B < 1 - \frac{1}{X} \tag{43}$$

However, this is only one criterion; we have seen that epidemic duration can also be unacceptable even though $R_B < 1$.

4.2.2. Equation for peak fraction of population infected: isolation-only

Again, for details on the methodology employed in the development of empirical equations see Appendix B.

For isolation applied alone, over the parameter ranges considered, we found i_{TMAX} contained within $1.39p_0 < i_{TMAX} < 3.2p_0$. This is much less variation than other metrics displayed in this study.

The empirical equation we developed for peak fraction of population infected at any one time is

$$i_{TMAX} = p_0(1 + R_0 g) \tag{44}$$

where

$$g = 0.228R_0 + 0.491\sigma_B - 0.459\sqrt{1 - R_B} \tag{45}$$

and

$$\sigma_B = \frac{\gamma_R}{\gamma_R + \gamma_B} \tag{46}$$

Over the test database, these equations have a mean absolute relative error of 4.9 percent and a maximum absolute relative error of 13.4 percent.

4.2.3. Equation for duration of epidemics controlled by isolation

Duration is highly sensitive to isolation reproduction number R_B. Fig. 4 showed earlier that T_E rises rapidly as $R_B \rightarrow 1$, suggesting the same $1/(1-R_B)$ relationship as we found for p_∞.

The form of the curves in Fig. 3 for large t suggests exponential decay. The linear analysis in Section 4.2.1 suggests it also. Then we can roughly model the curve late in time as

$$i(t) = i_0 \exp(-\lambda t) \tag{47}$$

Let the criterion for when an epidemic is extinguished be a threshold i_E on fraction of circulating population currently infected. Then

$$T_E = \frac{1}{\lambda} \ln\left(\frac{i_0}{i_E}\right) \tag{48}$$

If we accept i_{TMAX} (Eq. (44)) as a surrogate for i_0 then we might search for an equation in the form

$$T_E = \frac{f_1}{\gamma_R} \ln\left(f_2 \frac{i_{TMAX}}{i_E}\right) \tag{49}$$

where f_1 and f_2 are non-dimensional functions of the epidemic and control parameters.

Finally, numerical integration results show that T_E is inversely proportional to the basic reproduction number R_0. This is qualitatively consistent with duration in unmitigated epidemics; the more infectious the disease the shorter the epidemic.

Putting these findings together we ultimately arrive at the empirical equation

$$T_E = \frac{1.75 R_B}{R_0(1-R_B)\gamma_R} \ln\left(\frac{0.181 i_{TMAX}}{\sigma_B i_E}\right) \tag{50}$$

where i_{TMAX} is given by Eq. (44), σ_B by Eq. (46) and the threshold i_E is left as a choice for the user.

Over the test database, Eq. (50) has a mean absolute relative error of 10.4 percent and a maximum absolute relative error of 25.5 percent.

Together, Eqs. (15), (43) and (50) provide means to determine requirements on strength and speed of isolation to limit epidemic final size and duration to acceptable levels.

5. Dynamics of epidemic controlled by quarantine

This section explores dynamics of epidemic spread when controlled by quarantine.

We see quarantine as a time-driven process. We are modeling a homogeneous population but ought to take into account that governments differ and orders to quarantine can come from anywhere within the hierarchy of nation, state, county and city. Public officials wrestle with the decision; in time they issue an order, or do not, to the population as a whole; people comply individually, or do not, as time goes on. We combine the two activities into one process modeled, as we have said, by

Prob {person drawn at random from within the population is in quarantine at time t after start of the epidemic} =

$$q_A(t) = q_{A0}(1 - (1 + \gamma_A t)\exp(-\gamma_A t)) \tag{51}$$

The term $s(t)$ needed for the mass action law (Eq. (1)) is given by

$$s = 1 - p - q_{AS} \tag{52}$$

where

$q_{AS}(t)$ = prob{person is susceptible but well and in quarantine}.

From probability theory,

$$q_{AS}(t) = \int_0^t \dot{q}_A(\tau) s(\tau) d\tau = \int_0^t \dot{q}_A(\tau)(1 - p(\tau))d\tau \tag{53}$$

which we implement in the ODEs, using Eq. (51), by

$$\frac{dq_{AS}}{dt} = q_{A0}\gamma_A^2 t \exp(-\gamma_A t)(1 - p(t)) \tag{54}$$

The SIRAB model's use of non-time-invariant, or more simply, time-varying ODEs, i.e., where time appears explicitly on the right-hand side of equations for derivatives, has no counterpart in typical compartmental models; they are always time-invariant, though one sometimes sees piece-wise constant coefficients.

How do we compute the variable $i(t)$, the probability that a person is infected and in circulation? We can write

$$i = p - r - q_{AI} \tag{55}$$

For Eq. (55) to apply, the terms $r(t)$ and $q_{AI}(t)$ must be mutually exclusive. We must define $q_{AI}(t)$ to be the probability that a person was infected at some time τ, quarantined at a later time t_A, and has not recovered by time t. From that definition and probability theory,

$$q_{AI}(t) = \int_0^t \dot{q}(t_A) \int_0^{t_A} (1 - r(t|\tau))\dot{p}(\tau) d\tau dt_A \tag{56}$$

Hence

$$\frac{dq_{AI}}{dt} = \dot{q}_A \int_0^t (1 - r(t|\tau))\dot{p}(\tau) d\tau - \int_0^t \dot{q}(t_A) \int_0^{t_A} \frac{dr(t|\tau)}{dt} \dot{p}(\tau) d\tau dt_A \tag{57}$$

which becomes

$$\frac{dq_{AI}}{dt} = \dot{q}_A(p - r) - \int_0^t \dot{q}(t_A) \int_0^{t_A} \frac{dr(t|\tau)}{dt} \dot{p}(\tau) d\tau dt_A \tag{58}$$

The integral term is missing in Kalbaugh (2021). Because of the error that article's results for quarantine, and quarantine together with isolation, are incorrect.

With some work Eq. (58) can be shown to be equivalent to the following set of ODEs:

$$\begin{aligned}
\frac{dq_{AI}}{dt} &= \dot{q}_A(p - r) - \gamma_R J_1 \\
\frac{dJ_1}{dt} &= \dot{q}_A(r_1 - r) + \gamma_R(J_2 - J_1) \\
\frac{dJ_2}{dt} &= \dot{q}_A(p - r_1) - \gamma_R J_2 \\
\dot{q}_A &= q_{A0}\gamma_R^2 t \exp(-\gamma_R t)
\end{aligned} \tag{59}$$

These equations, together with

$$\begin{aligned}
\frac{dp}{dt} &= \beta s i \\
s &= 1 - p - q_{AS} \\
i &= p - r - q_{AI} \\
\frac{dr}{dt} &= \gamma_R(r_1 - r) \\
\frac{dr_1}{dt} &= \gamma_R(p - r_1) \\
\frac{dq_{AS}}{dt} &= \dot{q}_A(1 - p)
\end{aligned} \tag{60}$$

comprise the SIRAB model for epidemic dynamics when controlled by quarantine alone.

We have found empirically that, to a high degree of accuracy, the reproduction number for a quarantined-controlled epidemic in the SIRAB model is

$$R_A = R_0(1 - q_{A0}) \tag{61}$$

when $\gamma_A \geq \gamma_R$; i.e., when the rate of the process of quarantine is equal to or greater than the rate of recovery from the disease. Eq. (61) was analytically derived in Kalbaugh (2021) as applicable when the quarantine process is essentially completed before the fraction of infected people becomes appreciable. Our empirical results show that $\gamma_A \geq \gamma_R$ is sufficient for this to be the case when $R_A < 1$.

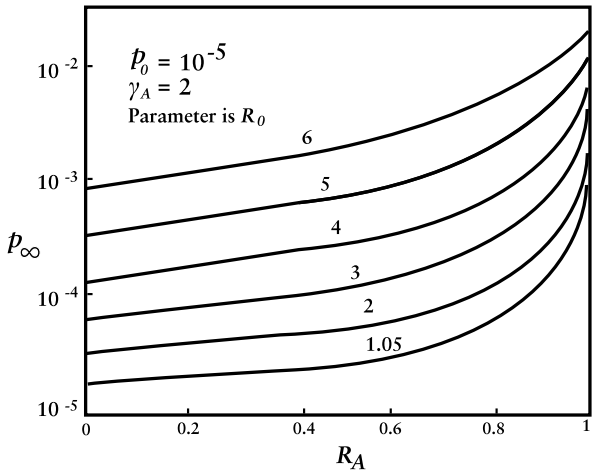

Fig. 5. Final size as a function of quarantine reproduction number, with basic disease reproduction number as a parameter.

5.1. Fundamentals of epidemic dynamics when controlled by quarantine

We begin discussion of epidemic dynamics when controlled by quarantine alone by exploring its qualitative nature, illustrating much of it graphically.

5.1.1. Final size: quarantine-only

Final size in an epidemic controlled by quarantine and final size in an epidemic controlled by isolation are alike in that they both grow rapidly as intervention reproduction number approaches unity. They differ in that p_∞ in the quarantine scenario depends strongly on basic disease reproduction number and on speed of intervention. Fig. 5 shows the dependence of p_∞ in the quarantine-only scenario as it depends on R_A (Eq. (61)) and R_0. Note that the logarithm of p_∞ appears to be approximately proportional to R_0.

5.1.2. Peak fraction of population infected: quarantine-only

In the quarantine-only scenario, i_{TMAX}, peak fraction of population infected, depends primarily on R_0 (though not to the same degree that p_∞ does) and only weakly on R_A. It is proportional to p_0 for $p_0 \leq 10^{-4}$. We saw these same dependencies for i_{TMAX} in the isolation-only scenario, but i_{TMAX} in the quarantine-only scenario is generally much larger than that in the isolation-only case.

It is in the behavior of i_{TMAX} that we can see most clearly the accuracy of Eq. (61) as the quarantine reproduction number. Fig. 6 shows that the slope of i_{TMAX} changes abruptly as q_{A0} goes through

$$q_{A0C} = 1 - 1/R_0 \tag{62}$$

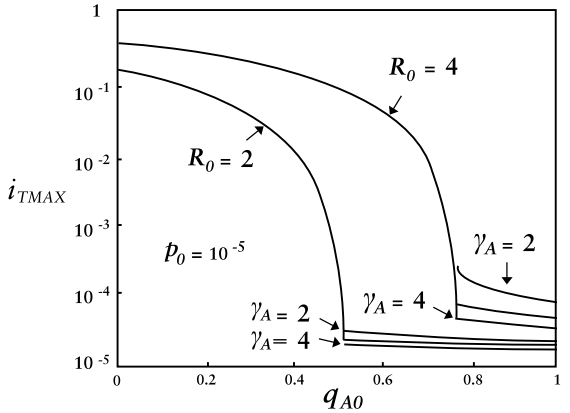

Fig. 6. Peak fraction of population infected as a function of quarantine strength, with quarantine speed and basic disease reproduction number as parameters.

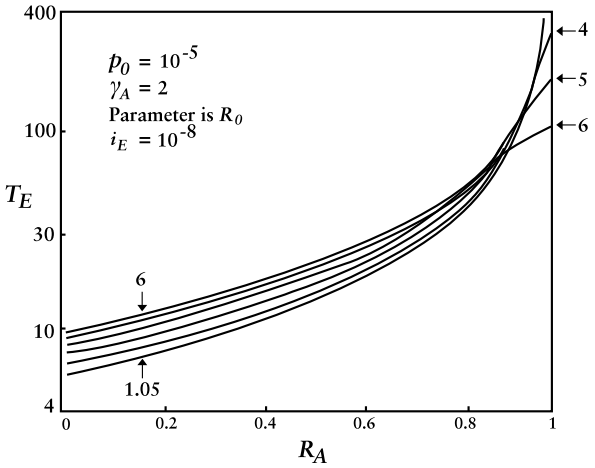

Fig. 7. Epidemic duration as a function of quarantine reproduction number with basic disease reproduction number as parameter.

and that these points are independent of γ_A.

To measure the accuracy of Eq. (61), we created a vector of 1000 evenly-spaced points along the q_{A0} line, defining

$$q_{A0}(n) = n/1000 \tag{63}$$

and computed i_{TMAX} for each of these points, over a test database of 64 cases: 8 values of R_0 ($1.05 \le R_0 \le 6$) and 8 values of γ_A ($2 \le \gamma_A \le 4$). We defined the numerically integrated q_{A0C} to be the value of $q_{A0}(m)$, where m is the value of the number n for which the discrete approximation of the second derivative

$$i_{TMAX}(n) - 2i_{TMAX}(n-1) + i_{TMAX}(n-2) \tag{64}$$

is a maximum. The mean absolute error between q_{A0C} computed this way and that given by Eq. (61) was $8.6 \cdot 10^{-5}$ and the maximum error was $6.3 \cdot 10^{-3}$.

5.1.3. Epidemic duration: quarantine-only

Fig. 7 shows the behavior of epidemic duration T_E as a function of the intervention reproduction number R_A and the basic disease reproduction number R_0. For low R_A, i.e., when the epidemic is well controlled, T_E increases with R_0. When R_A approaches unity, a reversal occurs: duration is shorter for larger R_0. The behavior of T_E as a function of γ_A is similar: T_E decreases with γ_A for low R_A and increases for high R_A. Duration also depends on the user's criterion for epidemic end.

5.2. Equations for quarantine performance metrics

Our intent in this section is to develop formulae for key performance metrics for an epidemic controlled by quarantine alone. We seek equations for p_∞, i_{TMAX} and T_E as a function of q_{A0}, γ_A, p_0 and R_0; empirical relations standing in for exact solutions we cannot expect to find.

Appendix B contains details of the development. We would have preferred to cover a wider range of parameter values, in particular higher values of R_0 and lower values of γ_A, because some diseases have R_0 values higher than 6 and history shows that quarantine orders and compliance are not always swift in coming, raising interest in $\gamma_A < \gamma_R$. However, in the SIRAB model, dynamic behavior for $R_0 > 6$ is increasingly difficult to model, and Eq. (61) ceases to apply for all values of R_0 considered here when $\gamma_A < \gamma_R$. Especially virulent epidemics and gradual application of quarantine require their own studies.

5.2.1. Equation for final size: quarantine-only

The empirical equation we have developed for final size in the region $0 \le R_A \le 0.9$ is

$$p_\infty = \left(\frac{p_0}{1 - R_A}\right) \exp(G_{AP}) H_{AP} \tag{65}$$

where

$$G_{AP} = 2.836R_0\sigma_A^2 - \left(0.745 - 0.538R_0\sigma_A^2\right)R_A$$
$$H_{AP} = \frac{\left(\sqrt{R_0}\,(1-R_A)+0.03\right)\left(1+0.0733\left(R_0-1\right)\right)}{\left(\sqrt{R_0}+2.20\sigma_A^2\right)\left(1-R_A+4.467\sqrt{p_0}\,R_0\sigma_A^2\right)} \tag{66}$$

R_A is given by Eq. (61) and

$$\sigma_A = \frac{\gamma_R}{\gamma_R+\gamma_A} \tag{67}$$

In Eq. (65), the term

$$\left(\frac{p_0}{1-R_A}\right)\exp(G_{AP})$$

is dominant; over the parameters of interest the multiplier H_{AP} is bounded by

$$0.66 \le H_{AP} \le 1.35 \tag{68}$$

Over the test database the mean relative absolute error in the above equations was 7.2 % and the maximum was 22.1 %. For the case where $R_A = 1$, we find that

$$p_\infty = 0.0707\sqrt{p_0}\exp(G_{AP1}) \tag{69}$$

where

$$G_{AP1} = 0.45 + 2.439\,\exp(-0.106(R_0-1)/\sigma_A) + 1.243(R_0-1)\sigma_A \tag{70}$$

has a mean relative absolute error of 4.4 % and maximum of 8.7 %. Note the dependence on $\sqrt{p_0}$ and recall Eq. (37).

5.2.2. Equation for peak fraction of population infected: quarantine-only

The equation we have developed for peak fraction of population infected in the quarantine-only scenario is

$$i_{TMAX} = 0.321p_0\,\exp(G_{AI})H_{AI} \tag{71}$$

where

$$G_{AI} = 1.972R_0\sigma_A^{\mu}(1+.0494R_0R_A)$$
$$H_{AI} = \frac{R_0\sigma_A+0.464}{R_0\sigma_A} \tag{72}$$
$$\mu = 1.39$$

and σ_A is given by Eq. (67). The mean relative absolute error was 7.7 % and the maximum was 25.1 %.

5.2.3. Equation for duration of epidemics controlled by quarantine

The equation we have developed for duration of an epidemic controlled by quarantine alone is

$$T_E = \frac{1.45}{\gamma_R}\ln\left(\frac{0.437i_{TMAX}}{\sigma_A i_E}\right)\,\frac{(1-a_1+a_2)(1-a_3)}{1-R_A+8.51\sqrt{p_0}R_0\sigma_A^2} \tag{73}$$

where

$$a_1 = 0.260\,\exp(-1.27(R_0+R_A-1))$$
$$a_2 = 0.285\,\exp(-2.36(1-R_A)) \tag{74}$$
$$a_3 = 1.37\,\exp(-17.3(7-R_0-R_A))$$

The mean relative absolute error was 7.5 % and the maximum was 23.8 %.

6. Dynamics of an epidemic controlled by isolation and quarantine

This section explores dynamics of epidemic spread when controlled by isolation and quarantine together.

As was the case for the SIRAB model's equations for dynamics of an epidemic controlled by quarantine alone, a key element here is the representation of the fraction of population infected and in circulation. We can write

$$i = p - r - q_B - q_{AI} \tag{75}$$

For Eq. (75) to apply, the probabilities r, q_B and q_{AI} must be mutually exclusive. We must define $q_{AI}(t)$ to be the probability that a person was infected at some time τ, not isolated prior to being quarantined at a later time t_A, and has not recovered by time t. From that definition and probability theory,

$$q_{AI}(t) = \int_0^t \dot{q}_A(t_A) \int_0^{t_A} (1 - q_B(t_A|\tau))(1 - r(t|\tau))\dot{p}(\tau) d\tau dt_A \tag{76}$$

where $\dot{p}(t)$, $r(t|\tau)$, $q_A(t)$ and $q_B(t|\tau)$ are given by Eq (1) through (4).

Then

$$\begin{aligned} \frac{dq_{AI}}{dt} = \dot{q}_A(t) \int_0^t (1 - q_B(t|\tau))(1 - r(t|\tau))\dot{p}(\tau) d\tau - \\ \int_0^t \dot{q}_A(t_A) \int_0^{t_A} (1 - q_B(t_A|\tau)) \frac{dr(t|\tau)}{dt} \dot{p}(\tau) d\tau dt_A \end{aligned} \tag{77}$$

We recognize that

$$\dot{q}_A(t) \int_0^t (1 - q_B(t|\tau))(1 - r(t|\tau))\dot{p}(\tau) d\tau = \dot{q}_A(p - r - q_B) \tag{78}$$

Now

$$1 - q_B(t_A|\tau) = 1 - q_{B0} + q_{B0}(1 + \gamma_B(t_A - \tau))\exp(-\gamma_B(t_A - \tau)) \tag{79}$$

so

$$\begin{aligned} \int_0^t \dot{q}_A(t_A) \int_0^{t_A} (1 - q_B(t_A|\tau)) \frac{dr(t|\tau)}{dt} \dot{p}(\tau) d\tau = \\ (1 - q_{B0}) \int_0^t \dot{q}_A(t_A) \int_0^{t_A} \frac{dr(t|\tau)}{dt} \dot{p}(\tau) d\tau + \\ q_{B0} \int_0^t \dot{q}_A(t_A) \int_0^{t_A} (1 + \gamma_B(t_A - \tau))\exp(-\gamma_B(t_A - \tau)) \frac{dr(t|\tau)}{dt} \dot{p}(\tau) d\tau dt_A \end{aligned} \tag{80}$$

We recognize the first term on the right hand side of Eq. (80) to be $(1 - q_{B0})$ times the integral term on the right hand side of Eq. (58), for which we have already found an equivalent set of ODEs (Eq (59)). Therefore it remains to find an equivalent set of ODEs for the final term in Eq. (80). With some work, these can be shown to be as given below in the full 14-state system of ODEs for the dynamics of epidemics controlled by both isolation and quarantine.

$$
\begin{aligned}
&\frac{dp}{dt} = \beta s i \\
&s = 1 - p - q_{AS} \\
&i = p - r - q_B - q_{AI} \\
&\frac{dr}{dt} = \gamma_R (r_1 - r) \\
&\frac{dr_1}{dt} = \gamma_R (p - r_1) \\
&q_B = i_B - q_{B0} r \\
&\frac{di_B}{dt} = (\gamma_R + \gamma_B)(i_{B1} - i_B) \\
&\frac{di_{B1}}{dt} = \left(\frac{\gamma_R^2 + \gamma_B^2}{\gamma_R + \gamma_B}\right) q_{B0} p + (\gamma_R + \gamma_B)(i_{B2} - i_{B1}) \\
&\frac{di_{B2}}{dt} = \left(\frac{2\gamma_R \gamma_B}{\gamma_R + \gamma_B}\right) q_{B0} p - (\gamma_R + \gamma_B) i_{B2} \\
&\dot{q}_A = q_{A0} \gamma_R^2 t \exp(-\gamma_R t) \\
&\frac{dq_{AS}}{dt} = \dot{q}_A (1 - p) \\
&\frac{dq_{AI}}{dt} = \dot{q}_A (p - r - q_B) - (1 - q_{B0}) \gamma_R J_1 - \gamma_R K_1 \\
&\frac{dJ_1}{dt} = \dot{q}_A (r_1 - r) + \gamma_R (J_2 - J_1) \\
&\frac{dJ_2}{dt} = \dot{q}_A (p - r_1) - \gamma_R J_2 \\
&\frac{dK_1}{dt} = \dot{q}_A (L_1 + L_2 - i_B) + \gamma_R (K_2 - K_1) \\
&\frac{dK_2}{dt} = \dot{q}_A (q_{B0} p - L_1 - L_2) - \gamma_R K_2 \\
&\frac{dL_1}{dt} = (\gamma_R + \gamma_B)\left(\left(\frac{\gamma_B}{\gamma_R}\right) L_2 - L_1\right) \\
&\frac{dL_2}{dt} = \gamma_R q_{B0} p - (\gamma_R + \gamma_B) L_2
\end{aligned}
\tag{81}
$$

Eq. (81) are fundamentally different from those in a typical compartmental model. Appendix C shows that the difference is numerically significant. Over a large test database, final size and peak fraction of population infected, taken together, were found to be on average about 75 % greater, and as much as 5 times greater, when calculated via SIRAB's ODEs, as compared to results of a typical compartmental model.

6.1. Fundamentals of epidemic dynamics when controlled by isolation and quarantine together

We begin this section with a number of time histories for epidemics controlled by both isolation and quarantine, to give a visual sense of their combined effects.

Fig. 8 shows that applying even a small quarantine effort in an epidemic only barely contained by isolation ($R_B = 0.9$) improves matters considerably. It graphs time histories of the probability that a person has been infected at some time during the epidemic for various added strengths of quarantine. And Fig. 9 shows that the converse is also true: a small isolation effort applied to an epidemic only barely contained by quarantine ($R_A = 0.9$) has significant positive effect.

The behavior of p_∞ and i_{TMAX} in the isolation-plus-quarantine scenario is qualitatively similar to that in the quarantine-only case. Epidemic duration, however, exhibits something new. As shown in Fig. 10, as combined intervention effort increases, T_E can drop abruptly to a duration floor which additional effort does little or nothing to reduce. This floor is in the low single digits of time units or less. (Again, the unit of time in this study is the mean recovery time.) Over the extensive T_E isolation-plus-quarantine test database, 15 percent of the durations were less than one unit and 32 percent were less than two.

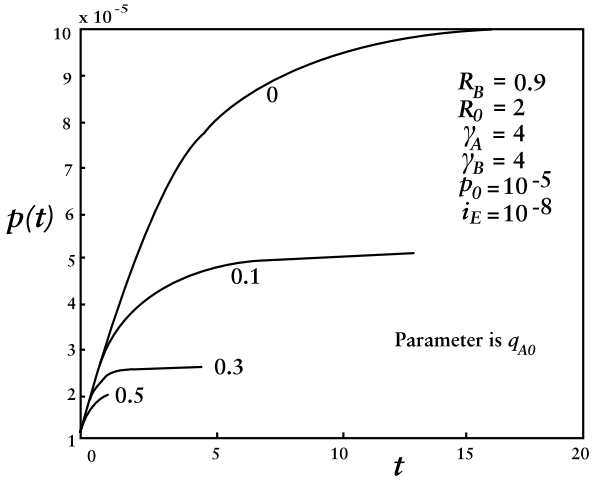

Fig. 8. Epidemic size as a function of time for an epidemic controlled primarily by isolation, with various levels of quarantine effort added.

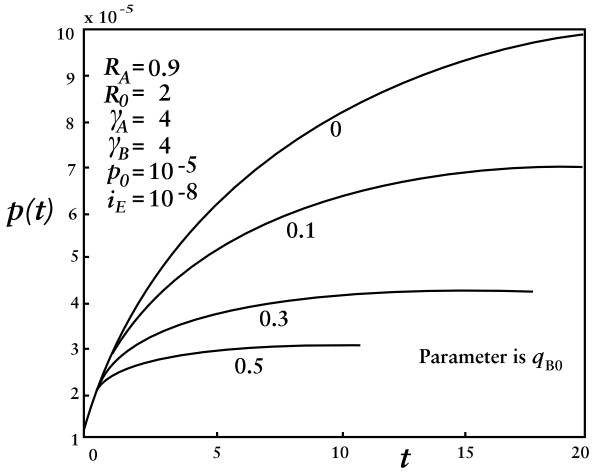

Fig. 9. Epidemic size as a function of time for an epidemic controlled primarily by quarantine, with various levels of isolation effort added.

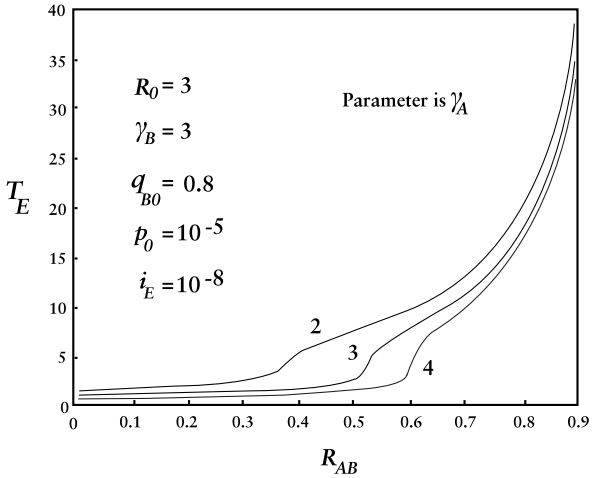

Fig. 10. Epidemic duration as a function of isolation-plus-quarantine reproduction number, with quarantine speed as parameter.

6.2. Equations for performance metrics: isolation and quarantine together

This section develops empirical equations for the key performance metrics when the epidemic is controlled by isolation and quarantine together.

Our task is eased by two observations. First, isolation is similar to recovery in its effect on epidemic spread. Second, when quarantine and isolation operate together quarantine is dominant. Therefore we might conceptually imagine the two processes operating sequentially rather than simultaneously: isolation reduces the reproduction number from R_0 to R_B and modeling joint behavior becomes a matter of replacing R_0 with R_B in equations for quarantine performance. As it happens, matching numerical integration results is not quite so simple, but the notion starts us down a productive path.

A success of the idea that one can replace R_0 with R_B in equations for quarantine performance to obtain equations for quarantine-plus-isolation performance is that the equation

$$R_{AB} = 1, \tag{82}$$

where

$$R_{AB} = R_B(1 - q_{A0}) \tag{83}$$

predicts the critical divide for a given R_B and γ_A with a mean absolute error of $3.1 \cdot 10^{-3}$ and maximum error of $2.0 \cdot 10^{-2}$ in q_{A0C} over the test database, using the same testing procedure as described in Section 5.1.2. Compare with Eq. (61) and the accuracy figures given in Section 5.1.2.

Our trials of replacing R_0 with R_B everywhere in the quarantine equations for p_∞, i_{TMAX} and T_E did not yield sufficiently accurate estimates of isolation-plus-quarantine performance. We found that values between R_B and R_0 were needed, in a proportion that depended on scenario parameters. We found through experimentation that R_0 should be replaced with a value R_E given by

$$R_E = cR_B + (1 - c)R_0 \tag{84}$$

where

$$c = \frac{R_C}{R_0 + R_C} \tag{85}$$

and

$$R_C = 0.5\sqrt{1 - R_{AB}}\Big/\sigma_B^2 \tag{86}$$

With this modification the functional forms we developed for p_∞ and i_{TMAX} in the quarantine scenario apply also to the isolation-plus-quarantine scenario, provided we tolerate somewhat larger errors. We believe the simplicity is worth the cost in accuracy. Coefficients and exponents applicable to the quarantine-only scenario needed to be modified.

The results:

For final size:

$$p_\infty = \left(\frac{p_0}{1 - R_{AB}}\right)\exp(G_{ABP})H_{ABP} \tag{87}$$

where

$$\begin{aligned} G_{ABP} &= 2.632R_E\sigma_A^2 - \left(1.274 - 0.7182R_E\sigma_A^2\right)R_{AB} \\ H_{ABP} &= \frac{\left(\sqrt{R_E}\,(1 - R_{AB}) + 0.0579\right)(1 + 0.0853(R_E - 1))}{\left(\sqrt{R_E} + 0.308\sigma_A^2\right)(1 - R_{AB} + 1.53\sqrt{p_0}\,R_E\sigma_A^2)} \end{aligned} \tag{88}$$

R_{AB} is given by Eq. (83) and σ_A, again, is given by Eq. (67).

Mean error: 9.9 % Maximum error 32.4 %.

For peak fraction of population infected:

$$i_{TMAX} = 0.587p_0\,\exp(G_{ABI})H_{ABI} \tag{89}$$

where

$$
\begin{aligned}
G_{ABI} &= 1.81 R_E \sigma_A^{\mu}(1 + 0.0535 R_E R_{AB}) \\
H_{ABI} &= \frac{R_E \sigma_A + 0.104}{R_E \sigma_A} \\
\mu &= 1.44
\end{aligned}
\tag{90}
$$

Mean error: 8.9 %. Maximum error: 27.9 %.

Developing a sufficiently accurate model for T_E required additional work because of the abrupt transition to a duration floor, as discussed in Section 6.1, which many simulation runs exhibited. Modeling accuracy depended on predicting the intervention effort, represented by $R_{AB} = R_B(1 - q_{A0})$, at which the transition occurs. The formula

$$
R_{ABT} = 0.85(R_0 \sigma_B / R_B)^{1.62} + R_0(W - XR_0)(1 + 0.0717 \log(1 / \sigma_A)) \tag{91}
$$

where

$$
\begin{aligned}
W &= 2.68 \cdot 10^{-2}(R_0 \sigma_B / R_B) \\
X &= 5.65 \cdot 10^{-3}(R_B / R_0)
\end{aligned}
\tag{92}
$$

had a mean absolute error of 0.10 and a maximum of 0.28 over the test database. See Appendix B for the test methodology. Over the test database, transitions did not occur ($R_{ABT} = 0$) if

$$
R_B \sigma_A / R_0 \geq 0.293 \tag{93}
$$

with a mean absolute error in the constant of 0.041 and a maximum of 0.070.

Then the equation for epidemic duration when both isolation and quarantine are applied is

$$
T_E = \left(\frac{6.6}{\gamma_R}\right)^{1-\nu} T_{EF}^{\nu} \tag{94}
$$

where

$$
\nu = \frac{1}{2}(1 + erf(0.957(R_{AB} - R_{ABT})) \tag{95}
$$

and

$$
\begin{aligned}
T_{EF} &= \frac{2.38}{\gamma_R} \ln\left(\frac{0.053 i_{TMAX}}{\sigma_A i_E}\right) H_T \\
H_T &= \max\left(0, \frac{(1 - a_{11} + a_{22})(1 - a_{33})}{1 - R_{AB} + 6.29\sqrt{p_0} R_E \sigma_A^2}\right) \\
a_{11} &= 0.396 \exp(-6.287(R_E + R_{AB} - 1)) \\
a_{22} &= 0.259 \exp(-2.421(1 - R_{AB})) \\
a_{33} &= 0.178 \exp(-8.99(7 - R_{AB} - R_E))
\end{aligned}
\tag{96}
$$

As combined intervention effort increases, R_{AB} decreases and the exponent ν goes rapidly from one to zero, effecting a transition from Eq. (96) to a duration floor of 3.3 time units. (Recall $\gamma_R = 2$ here.) Note that Eq. (96) have essentially the same functional form as in the quarantine-only scenario (Eq. (73)), with R_E replacing R_0.

For the short durations common in the combined isolation and quarantine scenario, relative error is untenable as an accuracy measure. For ODE-derived durations shorter than 10 time units, the mean absolute (i.e., non-relative) error was 1.1 units and the maximum 6.5 units. Over the extensive test database, 78 percent of durations were less than 10 time units. For ODE-derived durations longer than 10 units the mean relative error was 10.2 percent and the maximum 37.8 percent.

Another metric requiring special methods was final size when $R_{AB} = 1$. Replacing R_0 with R_E in Eq. (69) leads to an equation without parameters of isolation effort, while numerical integration results show that isolation has a strong effect. A different approach was needed. The result:

$$
p_{\infty} = 0.0421\sqrt{p_0} \exp(G_{ABP1}) \tag{97}
$$

where

$$G_{ABP1} = 1.803 \cdot b + (1.547/b)\exp(-0.141(R_0 - 1)/\sigma_A) + 1.077(R_0 - 1)\sigma_A$$
$$b = \left(\frac{R_B}{R_0}\right)^{\Gamma} \tag{98}$$
$$\Gamma = 0.102 \Big/ \sigma_A^2$$

Mean error: 8.5 % Maximum error: 25.1 %
Note the dependence on $\sqrt{p_0}$ and recall Eqs. (37) and (69).

7. Concluding remarks

The main results of this study are explicit closed-form equations for key metrics of epidemic control effectiveness as a function of intervention effort. As best we can determine, the literature has examples of implicit equations but not of equations in explicit form. We quantified the metrics of final size p_∞, peak fraction of population infected at any one time i_{TMAX}, and duration T_E. Tables 1 and 2 and 3 provide a summary. We solved analytically the differential equations for final size of an epidemic controlled by isolation alone when p_∞ is sufficiently small. In the other cases the equations were derived empirically. Table 4 defines reproduction numbers and quasi-reproduction numbers employed in the equations in Tables 1–3.

Among other key results.

- Isolation's effect on epidemic spread is similar to that of natural recovery from the disease. This can be exploited in modeling dynamics of isolation and quarantine operating together.
- When quarantine and isolation operate together quarantine is dominant. This too can be exploited in modeling of quarantine and isolation operating together.
- A small amount of quarantine effort can aid considerably in an epidemic only barely contained by isolation.
- A small amount of isolation effort can aid considerably in an epidemic only barely contained by quarantine.
- Over a large test database, final size and peak fraction of population infected, taken together, were found to be on average about 75 % greater, and as much as 5 times greater, when calculated via SIRAB's ODEs, as compared to results of a typical compartmental model.

Response to COVID 19 shows that simple models have a place. While national governments strove to rely on the most realistic models available, many studies were conducted, early on, using models with the same simplifications as in the SIRAB model (e.g., homogeneous population, deterministic ODEs and strong assumptions such as a person quarantined remains so for the duration of the epidemic) to project, albeit roughly, the course of the epidemic in a specific region and to provide a tentative assessment of candidate interventions. Simple models can also be used as plausibility checks, testing whether answers from large, complex computer calculations are within logical bounds. They can be useful introductory educational tools for those entering the epidemiology profession. Finally, as this article demonstrates, a simple model can quantify, with a broad brush, important metrics of intervention effectiveness parametrically, which is difficult to do with a complex model that has many parameters.

Among the SIRAB model's differences from typical compartmental models are.

- Incorporation of strength and speed of interventions rather than speed alone. This permits modeling imperfect intervention; e.g., weaknesses in contact tracing, or inconsistencies in quarantine orders and/or compliance.

Table 1
Equations for performance metrics in an epidemic controlled by isolation.

Metric	Equation	Mean Error (%)	Max Error (%)	Conditions
p_∞	$\frac{p_0}{1-R_B}$	–	0.6	$R_B \le 0.9$ $p_0 \le 10^{-4}$
	$\frac{p_0}{1-R_B+0.5\left(\frac{p_0}{1-R_B}\right)-4.1\left(\frac{p_0}{1-R_B}\right)^2}$	–	1.0	$R_B \le 0.98$ $p_0 \le 10^{-3}$
	$\sqrt{2p_0}$	–	1.5	$R_B = 1$ $p_0 \le 10^{-3}$
	$(2p_0)^{1/2} - (1/3)(2p_0) + (11/72)(2p_0)^{3/2} - (43/540)(2p_0)^2$	–	0.7	$R_B = 1$ $p_0 \le 0.2$
i_{TMAX}	$i_{TMAX} = p_0(1 + R_0 g)$ $g = 0.228R_0 + 0.491\sigma_B - 0.459\sqrt{1-R_B}$	4.9	13.4	$R_B \le 1$
T_E	$\frac{1.75R_B}{\gamma_R R_0(1-R_B)}\ln\left(\frac{0.181 i_{TMAX}}{\sigma_B i_E}\right)$	10.4	25.5	$R_B \le 0.9$

Table 2
Equations for performance metrics in an epidemic controlled by quarantine.

Metric	Equation	Mean Error (%)	Max Error (%)	Conditions
p_∞	$p_\infty = \left(\frac{p_0}{1-R_A}\right)\exp(G_{AP})H_{AP}$ $G_{AP} = 2.836R_0\sigma_A^2 - (0.745 - 0.538R_0\sigma_A^2)R_A$ $H_{AP} = \frac{(\sqrt{R_0}\,(1-R_A)+0.03)(1+0.0733(R_0-1))}{(\sqrt{R_0}+2.20\sigma_A^2)(1-R_A+4.467\sqrt{p_0}R_0\sigma_A^2)}$	7.2	22.1	$R_A \le 0.9$
	$p_\infty = 0.0707\sqrt{p_0}\exp(G_{AP1})\ G_{AP1} = 0.45 + 2.439\exp(-0.106(R_0-1)/\sigma_A) + 1.243(R_0-1)\sigma_A$	4.4	8.7	$R_A = 1.0$
i_{TMAX}	$i_{TMAX} = 0.321p_0\exp(G_{AI})H_{AI}$ $G_{AI} = 1.972R_0\sigma_A^{\mu}(1+0.0494R_0R_A)$ $H_{AI} = \frac{R_0\sigma_A + 0.464}{R_0\sigma_A}$ $\mu = 1.39$	7.7	25.1	$R_A \le 1.0$
T_E	$T_E = \frac{1.45}{\gamma_R}\ln\left(\frac{0.437i_{TMAX}}{\sigma_A i_E}\right)\ \frac{(1-a_1+a_2)(1-a_3)}{1-R_A+8.51\sqrt{p_0}R_0\sigma_A^2}$ $a_1 = 0.260\exp(-1.27(R_0+R_A-1))$ $a_2 = 0.285\exp(-2.36(1-R_A))$ $a_3 = 1.37\exp(-17.3(7-R_0-R_A))$	7.5	23.8	$R_A \le 0.9$

Table 3(a)
Equations for performance metrics in an epidemic controlled by isolation and quarantine.

Metric	Equation	Mean Error (%)	Max Error (%)	Conditions
p_∞	$p_\infty = \left(\frac{p_0}{1-R_{AB}}\right)\exp(G_{ABP})H_{ABP}$ $G_{ABP} = 2.632R_E\sigma_A^2 - (1.274 - 0.7182R_E\sigma_A^2)R_{AB}$ $H_{ABP} = \frac{(\sqrt{R_E}\,(1-R_{AB})+0.0579)(1+0.0853\cdot(R_E-1))}{(\sqrt{R_E}+0.308\sigma_A^2)(1-R_{AB}+1.53\sqrt{p_0}R_E\sigma_A^2)}$	9.9	32.4	$R_{AB} \le 0.9$
	$p_\infty = 0.0421\sqrt{p_0}\exp(G_{ABP1})$ $G_{ABP1} = 1.803\cdot b + (1.547/b)\exp(-0.141(R_0-1)/\sigma_A) + 1.077(R_0-1)\sigma_A$ $b = \left(\frac{R_B}{R_0}\right)^{\Gamma}$ $\Gamma = 0.102/\sigma_A^2$	8.5	25.1	$R_{AB} = 1.0$
i_{TMAX}	$i_{TMAX} = 0.587p_0\exp(G_{ABI})H_{ABI}$ $G_{ABI} = 1.81R_E\sigma_A^{\mu}(1+0.0535R_ER_{AB})$ $H_{ABI} = \frac{R_E\sigma_A + 0.104}{R_E\sigma_A}$ $\mu = 1.44$	8.9	27.9	$R_{AB} \le 1.0$

- Use of second order gamma distributions for recovery and intervention time to events, which have more realistic time profiles than do exponential distributions.
- Employment of non-time-invariant ODEs for quarantine.
- Accounting for removal of unexposed, susceptible individuals from circulation, an essential feature of quarantine.

All of the above can be included, one way or another, in a compartmental model, though they seldom or never are. These features may make the SIRAB model a more convenient and more realistic tool for broad brush analysis. Comparison with empirical field data is needed.

Another potential research direction: A reviewer has brought to our attention the artificial intelligence-based methodology *symbolic regression*. In the work documented in this article, in a process described in detail in Appendix B, we supplied the computer with a candidate functional form and the computer searched to find values for constants (coefficients and exponents) minimizing error between the equation and numerical integration results. In symbolic regression, based on data alone, the computer searches over both a wide range of functional forms and constants to minimize the error. It would be interesting to compare symbolic regression results with those of this article. Makke and Chawla (2024) and Angelis et al.

Table 3(b)
Equations for performance metrics in an epidemic controlled by isolation and quarantine.

Metric	Equation	Mean Error (%)	Max Error (%)	Conditions
T_E	$T_E = \left(\frac{6.6}{\gamma_R}\right)^{1-\nu} T_{EF}^{\nu}$ $\nu = \frac{1}{2}(1 + erf(0.9566(R_{AB} - R_{ABT}))$	1.1 time units $T_E \le 10$	6.5 time units $T_E \le 10$	$R_{AB} \le 0.9$
	$T_{EF} = \frac{2.38}{\gamma_R} \ln\left(\frac{0.053 i_{TMAX}}{\sigma_A i_E}\right) H_T$ $H_T = \max\left(0, \frac{(1 - a_{11} + a_{22})(1 - a_{33})}{1 - R_{AB} + 6.29\sqrt{p_0 R_E \sigma_A^2}}\right)$ $a_{11} = 0.396 \exp(-6.287(R_E + R_{AB} - 1))$ $a_{22} = 0.259 \exp(-2.421(1 - R_{AB}))$ $a_{33} = 0.178 \exp(-8.99(7 - R_{AB} - R_E))$	10.2 % $T_E > 10$	37.8 % $T_E > 10$	
	$R_{ABT} = 0.85(R_0 \sigma_B / R_B)^{1.62} +$ $R_0(W - XR_0)(1 + 0.0717 \log(1/\sigma_A))$ $W = 2.68 \cdot 10^{-2}(R_0 \sigma_B / R_B)$ $X = 5.65 \cdot 10^{-3}(R_B / R_0)$			

Table 4
Definitions of reproduction numbers and quasi-reproduction numbers.

Symbol	Equation	Intervention
R_A	$R_0(1 - q_{A0})$	Quarantine
R_B	$R_B = R_0\left[(1 - q_{B0}) + q_{B0}\left(\frac{\gamma_R}{\gamma_R + \gamma_B}\right)\left(1 + \frac{\gamma_R \gamma_B}{(\gamma_R + \gamma_B)^2}\right)\right]$	Isolation
R_{AB}	$R_B(1 - q_{A0})$	Quarantine plus isolation
R_E	$\left(\frac{R_C}{R_0 + R_C}\right) R_B + \left(\frac{R_0}{R_0 + R_C}\right) R_0$	Quarantine plus isolation
R_C	$R_C = 0.5\sqrt{1 - R_{AB}}/\sigma_B^2$	Quarantine plus isolation

(2023) are surveys of the current state of the art. Willem et al. (2014) is an application of symbolic regression to infectious disease modeling.

Declaration of competing interest

The authors declare that they have no known competing financial interests or personal relationships that could have appeared to influence the work reported in this paper.

Acknowledgement

We thank reviewers of this article and previous versions of it for their many constructive comments.

APPENDIX A

Assumptions Made in the SIRAB Model

In this Appendix we list important assumptions the SIRAB model makes.

- The population is homogenous.
- The population is large.
- In this article, births, deaths and immigration are ignored. In a separate section, Kalbaugh (2021) derived equations modifying the model to include them.
- No one is initially immune.

- A person who recovers is immune.
- Interaction times follow a homogeneous Poisson process.
- Deaths due to the epidemic are not an appreciable fraction of the population.
- A person quarantined remains so for the duration of the epidemic.
- Only a person who is currently infectious is subject to isolation.
- Contact rate is reduced in proportion to density of circulating population.

APPENDIX B

Methodology in Development of Empirical Equations

We analyzed three intervention scenarios: (1) isolation applied alone, (2) quarantine applied alone and (3) isolation and quarantine applied together. For each scenario the first step in the process was to develop a database with which to judge the accuracy of any candidate equation. For each scenario we developed a multi-variable grid of over many cases spanning a wide range of control parameter values, basic reproduction number values and initial conditions. Using MATLAB's ode15s algorithm we then numerically integrated the ODEs for each case and recorded p_∞, i_{TMAX} and T_E. These data were then employed to compute the mean and maximum absolute relative error for any candidate equation.

The first and most important step in equation development itself was to hypothesize a specific functional form of the equation, leaving coefficients to be determined later. We often graphed each metric as a function of each variable alone. We often had little idea of the form to expect so experimentation was important. We tried many different forms.

When a specific form looked attractive it was input to an assessment program. The search for optimum value of unknown constants was iterative, with wide searches followed by narrow ones. When constants for a specific functional form had been optimized but residual errors were still unacceptable we examined the error vector for its largest components and sought remedies for those differences in a new specific functional form.

B.1 Isolation Alone

From Eq. (15) we determine that, if the isolation process can achieve q_{B0} of 0.85 and γ_B of six, three times the rate of recovery, isolation alone can contain epidemics with R_0 of about 2.5. These appear to us to be challenging process goals. Nevertheless we set the range of parameters for study in this section to $1 < R_0 \leq 2.5$ and $1 \leq \gamma_B \leq 6$. To this we added $10^{-6} \leq p_0 \leq 10^{-4}$ and $0 \leq q_{BO} \leq 1$, provided $R_B < 1$ for i_{TMAX} and $R_B \leq 0.9$ for T_E.

The isolation test database for i_{TMAX} was 1610 cases of different combinations of these parameters. For T_E we added an additional parameter, the threshold i_E, $10^{-4}p_0 \leq i_E \leq 10^{-2}p_0$, provided $i_E \leq 10^{-9}$. The T_E isolation test database consisted of 2000 cases.

B.2 Quarantine Alone

The quarantine test database for p_∞ and i_{TMAX} comprised 1296 cases: $1.05 \leq R_0 \leq 6$, $2 \leq \gamma_A \leq 4$, $10^{-6} \leq p_0 \leq 10^{-4}$, and $0 \leq q_{A0} \leq 1$, provided $R_A \leq 0.9$ for p_∞ and $R_A < 1.0$ for i_{TMAX}. For T_E we added the threshold: $10^{-4}p_0 \leq i_E \leq 10^{-2}p_0$, provided $i_E \leq 10^{-9}$. Its R_A limit was 0.9. The T_E quarantine database was 3125 cases. The quarantine database for p_∞ when $R_A = 1.0$ was 512 cases. Its maximum p_0 was 10^{-3}.

B.3 Isolation and Quarantine Together

For isolation and quarantine together the test database for p_∞ and i_{TMAX} consisted of 4096 cases: $1.05 \leq R_0 \leq 6$, $2 \leq \gamma_A \leq 4$, $1 \leq \gamma_B \leq 6$, $0.2 \leq q_{BO} \leq 1$, $10^{-6} \leq p_0 \leq 10^{-4}$, and $0.2 \leq q_{A0} \leq 1$, provided $R_{AB} \leq 0.9$ for p_∞, and $R_{AB} \leq 1.0$ for i_{TMAX}. For T_E we added the threshold: $10^{-4}p_0 \leq i_E \leq 10^{-2}p_0$, provided $i_E \leq 10^{-9}$. Its R_{AB} limit was 0.9. The T_E isolation-plus-quarantine database was 6912 cases. To find the R_{AB} at which T_E abruptly transitions to a duration floor we employed the same technique as used in Section 5.1.2 (see Eq. (64)) to find points of maximum and minimum second derivatives in the ODE-derived T_E curve. We empirically derived the R_{ABT} equation from a database of 126 such cases. The threshold equation for when no transition can occur was derived from a set of 15 cases found by hand where the transition was just beginning to emerge. The isolation-plus-quarantine database for p_∞ when $R_{AB} = 1.0$ was 768 cases. Its maximum γ_B was 5 and its maximum p_0 was 10^{-3}.

APPENDIX C

Numerical Comparison with Typical Compartmental Model

This Appendix compares intervention metrics computed using the SIRAB model to those computed using a typical SIR compartmental model. Most compartmental models in the contemporary literature are more complicated than SIR, with at least an E compartment for exposed but not symptomatic and often more than one compartment for quarantine. But the SIRAB model was built on the SIR archetype and the typical compartmental model should be comparable.

The rates γ_R, γ_A and γ_B are defined here as they are in the main text. To compare fairly the SIRAB model, with its second order processes, to a typical compartmental model, and its first order processes, we must divide the above rates by 2 in the compartmental model. This makes the mean times to events in the two models the same. When compartmental models address imperfect interventions they do so in various ad hoc ways, e.g., including transitions out of the intervention compartments. In such a case it is unclear to us if it is possible to find transition rates that provide a given q_{A0} or q_{B0}. There are similar difficulties with other ad hoc models of imperfect interventions. Therefore, we will assume perfect interventions in this comparison.

With the above conditions, in the nomenclature of this article and in its ODE formulation (using p and r as state variables instead of s and i), a typical compartmental model is as follows:

$$\begin{aligned}
\dot{p} &= \beta s i \\
s &= 1 - p - q_{AS} \\
i &= p - r - q_B - q_{AI} \\
\dot{r} &= (\gamma_R/2)(p - r) \\
\dot{q}_B &= (\gamma_B/2) i - (\gamma_R/2) q_{\mathbf{B}} \\
\dot{q}_{AS} &= (\gamma_A/2) s \\
\dot{q}_{AI} &= (\gamma_A/2) i - (\gamma_R/2) q_{AI}
\end{aligned} \tag{C.1}$$

We compared the SIRAB model (Eq. (81)) to Eq. (C.1) in 1296 test cases: $1.05 \le R_0 \le 6, 2 \le \gamma_A \le 4, 1 \le \gamma_B \le 6, 10^{-6} \le p_0 \le 10^{-4}$. Let $p_\infty(c)$, $i_{TMAX}(c)$ and $T_E(c)$ be the metrics as computed from numerical integration of Eq. (C.1) and define

$$\begin{aligned}
\rho_P &= p_\infty / p_\infty(c) \\
\rho_I &= i_{TMAX} / i_{TMAX}(c) \\
\rho_T &= T_E / T_E(c)
\end{aligned} \tag{C.2}$$

Over the test database, we always found $p_\infty > p_\infty(c)$ and $i_{TMAX} > i_{TMAX}(c)$. We almost always found $T_E < T_E(c)$. The mean and maximum of ρ_P were 1.64 and 4.71. The mean and maximum of ρ_I were 1.89 and 5.56. The mean, maximum and minimum of ρ_T were 0.432, 1.10, and 0.270.

These results show that the SIRAB model's differences from the typical compartmental model are numerically significant.

References

Adam, D. (2020). Special report: The simulations driving the world's response to COVID-19. *Nature, 580*(7803).

Aleta, M., et al. (2020). Modeling the impact of testing, contact tracing and household quarantine on second waves of COVID-19. *Nature Human Behaviour, 4*.

Angelis, D., Sofos, F., & Karakasidis, T. (2023). Artificial intelligence in physical sciences: Symbolic regression trends and perspectives. *Archives of Computational Methods in Engineering, 30*.

Baronchelli, A. (2007). Nonequilibium phase transitions in negotiation dynamics. *Physical Review E - Statistical, Nonlinear and Soft Matter Physics, 76*(5), Article 051102.

Baxter, G., et al. (2015). Critical dynamics of the k-core pruning process. *Physical Review X, 5*(3), Article 031017.

Bernoulli, D. (1766). An attempt at a new analysis of the mortality caused by smallpox and the advantages of inoculation to prevent it. *Mem Math Phy Acad Roy Sci, Paris*.

Blower, S. (2004). (Review of) an attempt at a new analysis of the mortality caused by smallpox and the advantages of inoculation to prevent it. *Reviews in Medical Virology, 14*.

Brauer, F. (2017). Mathematical epidemiology: Past, present and future. *Infectious Disease Modeling, 2*(Issue 2).

Brooks – Pollock, E., Danon, L., Jombart, T., & Pellis, L. (2021). Modelling that shaped the early COVID-19 pandemic response in the UK. *Philosophical Transactions of the Royal Society B, 376*(Issue 1829).

Deikmann, O., Heesterbeek, H., & Britton, T. (2013). *Mathematical tools for understanding infectious disease dynamics*. Princeton University Press.

Feng, Z. (2007). Final and peak epidemic sizes for SEIR models with quarantine and isolation. *Mathematical Biosciences and Engineering, 4*(#4).

Ferguson, N. M., Cummings, D. A. T., Fraser, C., Cajka, J. C., Cooley, P. C., & Burke, D. S. (2006). Strategies for mitigating an influenza epidemic. *Nature*, 442.

German, T. C., Kadau, K., Longini, I. M., & Macken, C. A. (2006). Mitigation strategies for pandemic influenza in the US. *PNAS, 103*(15).

Giordano, G., et al. (2020). Modeling the COVID-19 epidemic and implementation of population-wide interventions in Italy. *Nature Medicine, 26*(6).

Gog, J., & Hollingsworth, T. D. (2021). Epidemic interventions: insights from classic results. *Philosophical Transactions of the Royal Society B, 376*(1829).

Gumel, A. B., et al. (2004). Modeling strategies for controlling SARS outbreaks. In , *B. Proceedings of the Royal Society of London* (p. 271).

Halloran, M. E., et al. (2008). Modeling target layered containment of an influenza epidemic in the US. *PNAS, 105*(12).

Hamer, W. H. (1906). Epidemic disease in England – the evidence of viability and of persistence. *The Lancet, 167*.

Heesterbeck, et al. (2015). Modeling infectious disease dynamics in the complex landscape of global health. *Science, 347*(6227).

Heesterbeck, JAP, & Roberts, M. G. (2015). How mathematical epidemiology became a field of biology. *Philosophical Transactions of the Royal Society*.

Hethcote, H., Zhein, M., & Shengbing, I. (2002). Effects of quarantine in six endemic models for infectious diseases. *Mathematical Biosciences, 180*.

Huang, C., et al. (2020). Clinical features of patients infected with 2019 novel coronavirus in Wuhan, China. *Lancet, 395*.

Huang, W., et al. (2021). Data-driven and machine-learning methods to project coronavirus disease 2019 pandemic trend in Eastern Mediterranean. *Frontiers in Public Health, 9*, Article 602353.

Jewell, N., et al. (2020). Caution warranted: Using the institute for health metrics and evaluation model for predicting the course of the COVID-19 pandemic. *Annals of Internal Medicine, August*.

Kalbaugh, D. (2021). Probabilistic model for control of an epidemic by isolation and quarantine. *Bulletin of Mathematical Biology, 83*(6), 63.

Kermack, W. O., & McKendrick, A. G. (1927). A contribution to the mathematical theory of epidemics. In , *115. Proceedings of the Royal Society, A* (p. 772).

Kretzschmar, M. (2020). Disease modeling for public health; added value, challenges and institutional constraints. *Journal of Public Health Policy, 41*.

Kucharski, A., et al. (2020). Effectiveness of isolation, testing, contact tracing and physical distancing on reducing transmission of SARS-cov-2 in different settings: A mathematical modeling study. *The Lancet, 20*(Issue 10).

Lessler and Cummings. (2016). Mechanistic models of infectious disease and their impact on public health. *American Journal of Epidemiology, 183*(Issue 5).

Lewis, B., et al. (2007). *Simulated pandemic influenza outbreaks in Chicago. Virginia Bioinformatics Institute*. Virginia Polytechnic Institute and State University, Tech. *Report NDSSL-TR-07-004*.
Lipsitch, M., et al. (2003). Transmission dynamics and control of severe acute respiratory syndrome. *Science, 300*(5627).
Liu, Z., et al. (2020). Predicting the cumulative number of cases for the COVID-19 epidemic in China from early data. *Mathematical Biosciences and Engineering*. https://doi.org/10.3934/mbe.2020172
Makke, N., & Chawla, S. (2024). Interpretable scientific discovery with symbolic regression: A review. *Artificial Intelligence Review, 57*.
Metcalf, C., et al. (2015). Six challenges in modeling for public health policy. *Epidemics, 10*.
Muyabi, et al. (2010). A cost-based comparison of quarantine strategies for new emerging diseases. *Mathematical Biosciences and Engineering, 7*(3).
Peak, C., et al. (2020). Individual quarantine versus active monitoring of contacts for the mitigation of COVID-19: A modeling study. *The Lancet, 20*(Issue 9).
Rainisch, G., et al. (2020). A dynamic modeling tool for estimating health care demand from the COVID-19 epidemic and evaluating population-wide interventions. *International Journal of Infectious Diseases, 96*.
Safi, M., & Gumel, A. (2013). Dynamics of a model with quarantine-adjusted incidence and quarantine of susceptible individuals. *Journal of Mathematical Analysis and Applications, 399*(2).
Sarkar, K., & Nieto, J. (2020). Modeling and forecasting the COVID-19 pandemic in India. *Chaos, Solitons & Fractals, 139*.
Siettos, C., & Russo, L. (2013). Mathematical modeling of infectious disease dynamics. *Virulence, 4*(4).
Stauffer, D., & Aharony, A. (2018). *Introduction to percolation theory*. Taylor & Francis.
Van Kerkhove, M., & Ferguson, N. (2012). Epidemic and intervention modeling – a scientific rationale for policy decisions? Lessons from the 2009 influenza pandemic. *Bulletin of the World Health Organization, 90*(4).
Willem, L., et al. (2014). Active learning to understand infectious disease models and improve policy making. *PLoS Computational Biology, 10*(4), Article e1003563.
Xu, Z., Song, J., Liu, W., et al. (2023). An agent-based model with antibody dynamics information in COVID-19 epidemic simulation. *Infectious Disease Modelling, 8*(4).
Zhang, Y., Arenas, A., & Yagan, O. (2018). Cascading failures in interdependent systems under a flow redistribution model. *Physical Review E, 97*(2), Article 022307.